

three reversible waves, suggesting that it has a uniform and simple structure and excellent stability in the electrochemical sense. A relevant study of the copper complex derived from the optically active octameric ligand $[\text{CH}_2\text{CH}(\text{CH}_3)\text{N}(\text{CONHPh})]_{n=8}$ ^{10c,19} showed typical copper bands with diffused fine structures, corresponding to essentially "square-planar" configuration in the CD spectrum.

The iron(III) complex **2** was similarly prepared by mixing octameric ligand (0.19 unit mmol) and iron(III) chloride (0.030 mmol) in 30 mL of methanol-methylene chloride solution (1:1, v/v) for 4 h. After removal of solvent, the methylene chloride soluble fraction (ca. 85%) was used. This complex was yellow red but exhibited no discrete absorption maximum in the methylene chloride. Although its coordination chemistry is not clear at present, it shows highly lipophilic properties, enough to be soluble in the used liquid membrane.

Other copper complexes **3-7** were synthesized according to literature methods.²⁰

Transport Experiments. The passive transport experiments (Tables I and II) were carried out at room temperature (ca. 15 °C) in a similar apparatus as described before.¹³ A cylindrical glass cell (4.0 cm, i.d.) holds a glass tube (2.0 cm, i.d.) that separates two aqueous phases. Typically, the inner aqueous phase (aqueous phase I) contains substrate anion in 4 mL of alkaline solution. The outer phase (aqueous phase II) contains antiport anion in 10 mL of water. The membrane layer (8 mL of methylene chloride), in which carrier is dissolved, lies below these two aqueous phases and bridges the separation by the central glass tube. This methylene chloride layer is stirred by a magnetic stirrer. Although we confirmed that the variations in stirring speed had no pronounced effect on the transport rates, the transport phenomena were not found to occur without any perturbations.

A similar transport experiment with each substrate anion was performed in the absence of carrier for reference, and leakage of substrate

was found to be very small ($\sim 0.1 \times 10^{-6}$ mol/h).

The substrate anion concentration in aqueous phase II was confirmed to increase linearly with running time (<16 h), and the initial rates are shown in the tables.

The antiport anion was also observed to move from aqueous phase II to I. When the perchlorate anion was employed as antiport anion, we found that the amount of perchlorate anion transported, determined by the methylene blue method,²¹ was almost equal to that of substrate anion transferred under the conditions stated in Tables I and IV. The detailed conditions are included in each table.

The active transport of amino acid derivatives was performed in a U-shaped glass cell (2.0 cm, i.d.). The carrier in methylene chloride (12 mL) is placed in the base of the cell, and two aqueous phases (5 mL each) of equal substrate concentration and pH are placed in the arms of the cell, floating on the methylene chloride. The membrane phase is stirred constantly by a magnetic stirrer.

When the salt of antiport anion (KCl, NaClO_4 , or KSCN) was added in aqueous phase II, substrate anion was transported from aqueous phase I to II. The concentration of substrate anion in aqueous phase I increased with running time and reached a steady state (usually after 20 h). The concentration of substrate anion in aqueous phase I also decreased at an almost similar rate.

Liquid-Liquid Extraction Experiments. The methylene chloride solution of carrier was allowed to contact an aqueous solution of sodium salt of substrate anion. After a given period (ca. 1 h), an organic phase was separated from aqueous phase. The extracted amount of substrate anion was calculated from the difference between the concentrations of initially and remaining substrate anion in the aqueous phase. The detailed conditions are included in Table II.

Registry No. **3**, 55997-76-7; **4**, 82469-60-1; **5**, 82469-61-2; **6**, 46369-53-3; **7**, 10380-28-6; **8**, 5137-55-3; $[\text{CH}_2\text{CH}_2\text{N}(\text{CSNHPh})]_m$ 71093-49-7; copper(II) chloride, 7447-39-4; iron(III) chloride, 7705-08-0.

(21) Boltz, D. F. "Colorimetric Determination of Non-Metals"; Interscience: New York, 1958; p 176.

(19) Araki, T.; Nagata, K.; Tsukube, H. *J. Polym. Sci., Polym. Chem. Ed.* **1979**, *17*, 731-746.

(20) (a) Nakatsuka, Y. *Bull. Chem. Soc. Jpn.* **1936**, *11*, 45-48. (b) Jones, M. M. *J. Am. Chem. Soc.* **1959**, *81*, 3188-3189.

Proton NMR Characterization of the State of Protonation of the Axial Imidazole in Reduced Horseradish Peroxidase

Gerd N. La Mar* and Jeffrey S. de Ropp

Contribution from the Department of Chemistry, University of California, Davis, California 95616. Received August 3, 1981

Abstract: The detection of a single proton exchangeable resonance for unligated ferrous horseradish peroxidase, HRP, with hyperfine shift comparable to that found for the proximal histidyl imidazole $\text{N}_\epsilon\text{H}$ in deoxy myoglobins, hemoglobin, and models established that the axial imidazole in ferrous HRP, contrary to the interpretations of other spectroscopic evidence, is not deprotonated. A protein conformational change modulated by another titratable residue induces a significant change in the $\text{N}_\epsilon\text{H}$ contact shift. We show that simultaneous consideration of changes of the proximal histidyl imidazole $\text{N}_\epsilon\text{H}$ contact shift and resonance Raman $\nu(\text{Fe}-\text{N}_\epsilon)$ permit the differentiation between steric and electronic influences on iron-imidazole bonding. For ferrous HRP, the acid \rightarrow alkaline transition involves primarily changes in $\text{N}_\epsilon\text{H}$ hydrogen bonding to a peptide acceptor, with the degree of imidazolate character for the axial ligand slightly larger for the acid than for the alkaline form of the protein.

The proposal that electronic control of iron reactivity in hemoproteins is exercised primarily through the axial ligand is a cornerstone of the theories for the mechanism of action of both hemoglobins and heme peroxidases. The original Perutz model for hemoglobin cooperativity emphasized strained or stretched iron-histidine bonds.¹ More recently, recognition has been given to the fact that the strength of the iron-imidazole bond can be modulated indirectly by the formation of a hydrogen bond between the proximal histidyl imidazole $\text{N}_\epsilon\text{H}$ (A in Figure 1) and a protein

acceptor residue.²⁻⁶ Increased donor properties of the $\text{N}_\epsilon\text{H}$ would increase the imidazole σ basicity and hence strengthen the iron-imidazole bond.³ Even complete deprotonation of the imidazole in hemoglobin has been considered on the basis of ESR data,^{3,4}

(2) Morrison, M.; Schonbaum, G. R. *Annu. Rev. Biochem.* **1976**, *45*, 86-127. Nickolls, P. *Biochim. Biophys. Acta* **1962**, *60*, 217-228.

(3) Peisach, J. *Ann. N.Y. Acad. Sci.* **1975**, *244*, 187-202.

(4) Chevlon, M.; Salhany, J. M.; Castillo, C. L.; Peisach, J.; Blumberg, W. E. *Isr. J. Chem.* **1977**, *15*, 311-317.

(5) Swartz, J. C.; Stanford, M. A.; Moy, J. N.; Hoffman, B. M.; Valentine, J. S. *J. Am. Chem. Soc.* **1979**, *101*, 3396-3398.

(6) Valentine, J. S.; Sheridan, R. P.; Allen, L. C.; Kahn, P. *Proc. Natl. Acad. Sci. U.S.A.* **1979**, *76*, 1009-1013.

(1) Perutz, M. F.; Ten Eyck, L. F. *Cold Spring Harbor Symp. Quant. Biol.* **1971**, *36*, 295-310.

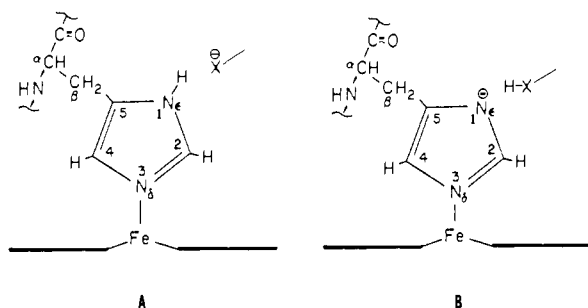


Figure 1. (A) Proximal histidyl imidazole shown with $N_{\epsilon}H$ essentially not interacting with protein H-bond acceptor X^{-} ; (B) proximal histidyl imidazolate formed by deprotonation of N_{ϵ} via transfer to X^{-} .

and studies on model compounds have revealed that deprotonation of an imidazole significantly alters their CO affinities.⁷ In the case of the present protein of interest, horseradish peroxidase, HRP, the unusual stability of higher oxidation states of iron has led to the proposal that the imidazole is deprotonated in several of its forms.² This view appears to be supported by recent optical spectra of unligated and CO-ligated ferrous porphyrins containing the ionized imidazolite ion, which differ from those of myoglobin but strongly resemble those of ferrous HRP and ferrous HRP-CO.⁸

Other evidence cited to support a deprotonated imidazole is the high $\nu(Fe-N_{\delta})$ relative to deoxymyoglobin as found in resonance Raman spectra.^{9,10} Moreover, the variable extent of hydrogen-bond acceptor strength of solvents has been shown to significantly influence $\nu(Fe-N_{\delta})$ leading to the suggestion that variable degrees of $N_{\epsilon}-H$ hydrogen bonding in the alternative quaternary states of hemoglobin may be primarily responsible for the energy of cooperativity.⁹

Among the many solution spectroscopic methods applied to hemoproteins, none have provided the structural details available from proton NMR or resonance Raman spectroscopy. For the high-spin five-coordinate ferrous hemoproteins, these two spectroscopic techniques provide particularly valuable insight into the structure of hemoproteins in that they are unique in detecting the state of the proximal histidyl imidazole considered crucial to the control of iron reactivity. Resonance Raman (RR) spectroscopy provides a direct measure of the iron-imidazole bond strength^{9,10,13,14} via $\nu(Fe-N_{\delta})$ (see Figure 1). Proton NMR, on the other hand, provides the only direct probe of the imidazole exchangeable ($N_{\epsilon}H$) proton, and the nature of its hyperfine shift¹⁵⁻¹⁹ clearly establishes the state of protonation of the axial imidazole. This $N_{\epsilon}-H$ hyperfine shift has been shown to reflect overwhelmingly a contact interaction resulting from iron spin

Table I. Steric vs. Electronic Influences on Bond Distances and Resonance Raman and Proton NMR Iron-Imidazole Spectral Parameters

influence		$r(Fe-N_{\delta})$	$\nu(Fe-N_{\delta})$	$N_{\epsilon}-H$ contact shift
steric	bond compression	decrease	increase	increase
	bond extension	increase	decrease	decrease
electronic (H bonding)	stronger H bond	decrease	increase	decrease
	weaker H bond	increase	decrease	increase

transfer into the imidazole σ system.^{11,15,16,18-20} However, while it is simple by NMR to establish that the imidazole is not deprotonated, it is less obvious though more interesting as to how to establish the presence of hydrogen bonding between the $N_{\epsilon}-H$ and some as yet unspecified acceptor residue.

While neither RR or NMR spectroscopy yields unambiguous interpretation of changes in their parameters in terms of dominant electronic or steric influences on the iron-imidazole bond, we show here that simultaneous consideration of the RR $\nu(Fe-N_{\delta})$ and the proton NMR $N_{\epsilon}-H$ contact shift permit one to identify the more likely dominant mechanism that is responsible for changes in these parameters during a protein conformational change. Such a protein conformational change, modulated by a single proton with $pK \sim 7$, has been characterized for reduced HRP by a number of physicochemical means.^{9,21} Although a physiological role for unligated ferrous HRP has only been suggested, the oxygenated complex, also called compound III, appears to exist under certain conditions.²²

Differentiation between simple steric (bond strain) and electronic influences via variable H bonding of the $N_{\epsilon}H$ can be made on the basis of the following simplified but intuitively reasonable hypothesis. As listed in Table I, extension (or compression) of the $Fe-N_{\delta}$ bond due to steric influences leads to a longer (shorter) $Fe-N_{\delta}$ bond and hence to a reduction (or increase) in the RR $\nu(Fe-N_{\delta})$ located in the 200-250- cm^{-1} region.^{9,10,13,14} In the case of variable H bonding of $N_{\epsilon}-H$, it is instructive to consider the limits of no H bonding and complete deprotonation. In the former case, the $N_{\epsilon}H$ hyperfine shift, which has been shown to arise overwhelmingly from contact shifts due to unpaired spin in the system,^{11,15,16,20} would be expected in the region 70-90 ppm, as found in both models^{15,16} and deoxymyoglobins^{16,19} in which neither axial tension nor H bonding influences are considered important. Upon complete deprotonation, the resulting imidazolate is a somewhat stronger σ base than neutral imidazole,^{8,10} leading to a fractional increase in the σ contact shift for the axial ligand as well as an increased $\nu(Fe-N_{\delta})$ due to the stronger bond. The deprotonation of $N_{\epsilon}H$, however, necessarily *completely severs the interaction* between the proton and the unpaired spin density on the coordinated imidazolate (B in Figure 1). Hence, while the amount of transferred σ spin to the imidazolate must increase, the subsequent transfer of spin density to the removed proton is completely terminated.²³ Thus for any intermediate case in which there is a significant partial removal of the $N_{\epsilon}H$ via partial proton donation to some hydrogen acceptor, the fractional decrease in the interaction of the $N_{\epsilon}H$ with the imidazole spin density is likely to be larger than the fractional increase in the extent of $Fe \rightarrow N_{\delta} \sigma$ spin transfer, as summarized in Table I. In the case of very weak H bonding, the contribution of direct spin transfer and spin polarization²⁰ could interfere with such a simple interpretation,

(7) Stanford, M. A.; Swartz, J. C.; Phillips, T. E.; Hoffman, B. M. *J. Am. Chem. Soc.* **1980**, *102*, 4492-4499.

(8) Mincey, T.; Traylor, T. G. *J. Am. Chem. Soc.* **1979**, *101*, 765-766.

(9) Teroaka, J.; Kitagawa, T. *Biochem. Biophys. Res. Commun.* **1980**, *93*, 694-700.

(10) Stein, P.; Mitchell, M.; Spiro, T. G. *J. Am. Chem. Soc.* **1980**, *102*, 7795-7797.

(11) La Mar, G. N. In "Biological Application of Magnetic Resonance"; Shulman, R. G., Ed.; Academic Press: New York, pp 305-343.

(12) Felton, R. H.; Yu, N.-T. In "The Porphyrins"; Dolphin, D., Ed.; Academic Press: New York, 1978; pp 347-293.

(13) (a) Kitagawa, T.; Nagai, K.; Tsubaki, M. *FEBS Lett.* **1979**, *104*, 376-378. (b) Nagai, K.; Kitagawa, T.; Morimoto, H. *J. Mol. Biol.* **1980**, *136*, 271-289. (c) Hori, H.; Kitagawa, T. *J. Am. Chem. Soc.* **1980**, *102*, 3608-3613.

(14) Kincaid, J.; Stein, P.; Spiro, T. G. *Proc. Natl. Acad. Sci. U.S.A.* **1979**, *76*, 549-552, 4156.

(15) Goff, H.; La Mar, G. N. *J. Am. Chem. Soc.* **1977**, *99*, 6599-6606.

(16) La Mar, G. N.; Budd, D. L.; Goff, H. *Biochem. Biophys. Res. Commun.* **1977**, *77*, 104-110.

(17) La Mar, G. N.; Nagai, K.; Jue, T.; Budd, D. L.; Gersonde, K.; Sick, H.; Kagimoto, T.; Hayashi, A.; Taketa, F. *Biochem. Biophys. Res. Commun.* **1980**, *96*, 1172-1177.

(18) La Mar, G. N.; Budd, D. L.; Sick, H.; Gersonde, K. *Biochim. Biophys. Acta* **1978**, *537*, 270-283.

(19) La Mar, G. N.; Anderson, R. R.; Budd, D. L.; Smith, K. M.; Langry, K. C.; Gersonde, K.; Sick, H. *Biochemistry*, **1981**, *20*, 4429.

(20) La Mar, G. N. In "NMR of Paramagnetic Molecules"; La Mar, G. N., Horrocks, W. D., Jr., Holm, R. H., Eds.; Academic Press: New York, 1973; Chapter 3.

(21) Yamasaki, I.; Arai, T.; Hayashi, Y.; Yamada, H.; Makino, R. *Adv. Biophys.* **1978**, *11*, 249-281.

(22) Yamasaki, I.; Yukota, K. *Mol. Cell. Biochem.* **1973**, *2*, 39-52.

(23) Ideally, the increase in $Fe-N_{\delta} \sigma$ covalency upon deprotonation could be directly monitored by observing the hyperfine shift changes of the 2-H and 4-H imidazole protons. While these are observable in imidazole models, such NMR data on imidazolate are not yet available. While the 2,4-H imidazole proton in deoxymyoglobin^{16,19} and monomeric deoxyhemoglobin¹⁸ have been detected, their expected extensive line width makes detection in large hemoproteins such as reduced HRP extremely unlikely.

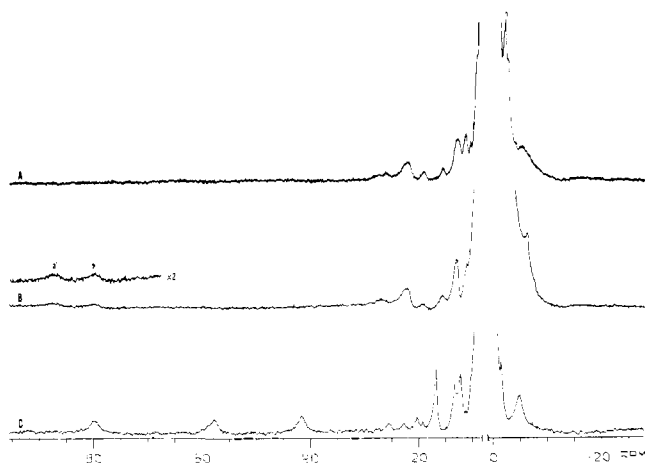


Figure 2. Traces of the 200-MHz proton NMR spectra at 25 °C of (A) ferrous HRP in $^2\text{H}_2\text{O}$, "pH" 7.8; (B) ferrous HRP in 90% $\text{H}_2\text{O}/10\%$ $^2\text{H}_2\text{O}$, pH 7.5; and (C) deuterohemin-reconstituted ferrous HRP, pH 9.4, in 90% $\text{H}_2\text{O}/10\%$ $^2\text{H}_2\text{O}$.

and shifts of the N_αH hyperfine shift and the RR $\nu(\text{Fe}-\text{N}_\delta)$ could be in the same direction.

Thus, changes in the opposite direction of the N_αH hyperfine shift and the resonance Raman $\nu(\text{Fe}-\text{N}_\delta)$ necessarily dictate that the change in iron reactivity originates in changes in N_αH hydrogen bonding rather than changes in Fe-imidazole steric strain.

Experimental Section

Horseradish peroxidase type VI was purchased as a lyophilized salt-free powder from Sigma Chemical Co. The purification, activity assay, and electrophoretic behavior of the HRP used in this study have been described elsewhere.²⁴ Preparation of deuterohemin reconstituted HRP, deuteroheme-HRP, from apo-HRP was also described elsewhere.²⁴ The ferrous form of the proteins was generated by addition of excess sodium dithionite under N_2 .

Solutions for proton NMR studies were 1–3 mM in protein in either 0.2 M NaCl, 99.8% $^2\text{H}_2\text{O}$, or 90% $\text{H}_2\text{O}/10\%$ $^2\text{H}_2\text{O}$. The solution pH, adjusted under N_2 with 0.2 M ^2HCl or 0.2 M NaOH , was measured with a Beckman 3550 pH meter equipped with an Ingold microcombination electrode. The pH was not corrected for the isotope effect and is hence referred to as "pH".

The 200-MHz proton NMR spectra were recorded on a Nicolet NT-200 Fourier transform NMR spectrometer operating with quadrature detection. Typical spectra consisted of 5000–10000 pulses with 4000 data points over a 40000-Hz bandwidth ($5 \mu\text{s}$ 90° pulse). The water peak was suppressed by an ca. 25-ms presaturation pulse; signal-to-noise was improved by exponential apodization, which introduced 10-Hz line broadening. Peak shifts were referenced to the residual water line, which in turn was calibrated against internal 4,4-dimethyl-4-silapentane-sulfonate, DSS. Chemical shifts are reported in parts per million, ppm, referenced to DSS, with downfield shifts positive; line widths are given in hertz.

Results and Discussion

The 200-MHz proton NMR spectra of reduced HRP at 25 °C in $^2\text{H}_2\text{O}$, "pH" 7.4, and 90% $\text{H}_2\text{O}/10\%$ $^2\text{H}_2\text{O}$, pH 7.5, are illustrated in A and B of Figure 2. Also included in this figure is the 25 °C, pH 9.4, trace for reduced deuteroheme-HRP in 90% $\text{H}_2\text{O}/10\%$ $^2\text{H}_2\text{O}$ (C). The spectrum in B is for a sample kept over 24 h in $^2\text{H}_2\text{O}$. When one compares the neutral pH traces in A and B of Figure 2, it is obvious that, in addition to numerous nonexchangeable peaks arising primarily from the heme and possibly some distal amino acid side chain, there are two exchangeable peaks, designated a and a', in the region 75–90 ppm. A single such exchangeable peak is also found in deuteroheme-HRP at high pH (C in Figure 2); the trace for the equilibrated protein in $^2\text{H}_2\text{O}$ is not shown, and the reduced form of this reconstituted protein is unsufficiently stable to obtain spectra reasonably quickly at much lower pH. The exchangeable peaks a, a' in Figure 2 exchange with solvent sufficiently slowly so that

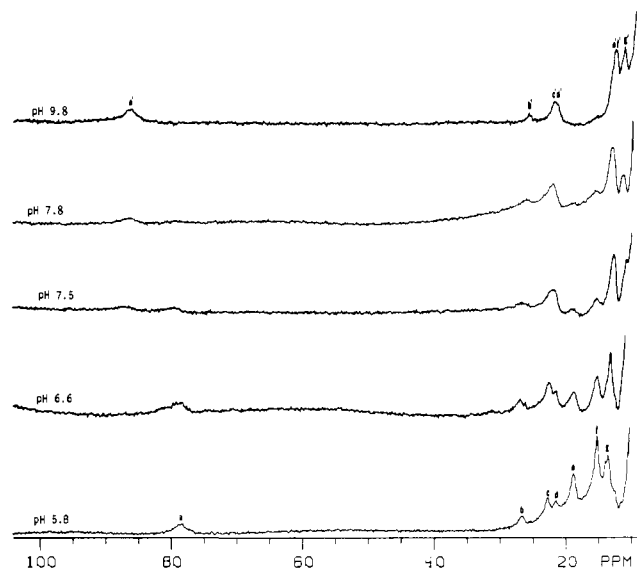


Figure 3. Downfield portions of the 200-MHz proton NMR spectra of ferrous HRP in 90% $\text{H}_2\text{O}/10\%$ $^2\text{H}_2\text{O}$ at 25 °C at the indicated pH values. The peaks are labeled a–g for the acid form and a'–g' for the alkaline form. Assignments²⁶ for acid and alkaline forms are c, d' (vinyl H_α); e, e' (5- CH_3); f, g' (8- CH_3); g, f' (3- CH_3).

dissolution of the protein lyophilized from H_2O and quickly dissolved in $^2\text{H}_2\text{O}$ yields essentially the full intensity of peaks a, a' for up to 1 h. Hence the pH and temperature dependence of the exchangeable resonances can be studied either in H_2O solution or in freshly prepared $^2\text{H}_2\text{O}$ solution.²⁵

In Figure 3 we present the downfield portions of the 200-MHz proton NMR spectra of reduced HRP in H_2O as a function of pH from 5.8 to 9.8. All peaks can be accounted for by two pH-interconvertible protein forms with the peaks for the dominant species in acid-to-neutral pH designated a–g and those arising from the main species at alkaline pH as a'–g', with the pair a, a' being the sole resolved exchangeable peaks for each protein form. Exchange between the two forms is slow on the NMR time scale, i.e., $\ll 20 \text{ s}^{-1}$ for methyl e. We have elsewhere carried out systematic deuteration labeling of several heme resonances of several ferrous hemoproteins.²⁶ Although little structural information could be gleaned from the assigned heme resonances,²⁶ the known assignments are included in the captions to Figure 3 for completeness. The three upfield peaks, h, i, and j in the alkaline form (A in Figure 2), have shifts essentially independent of the conformational transition. Integration of individual methyl resonances or the exchangeable peak a, a' as a function of "pH" yields a "pK" of 7.5, which is consistent with values obtained by other methods.^{9,21} The origin of the titrating residue responsible for this protein conformational change is not known but is generally believed to be the second and presumed distal histidine.²¹ The proton NMR data shed no further light on this matter except to definitely exclude the titration of the proximal histidine.

The unit proton intensity of both a and a' for each of the proteins is established by their relative intensities to the assigned methyls for each component at higher temperature where all lines are narrower and better resolved (not shown). This is further supported for reduced deuteroheme-HRP, whose single proton 2,4-H peaks appear at 41 and 57 ppm from DSS and have the same intensity as a'. These deuteroheme 2,4-H peaks resonate essentially in the same region as found in ferrous models,¹⁶ deoxyhemoglobins,^{11,19} and monomeric hemoglobins.¹⁸ The close similarity of the hyperfine shift pattern for the heme resonances in reduced HRP and deuteroheme-HRP and other characterized deoxyhemoproteins supports their great similarity in electronic

(25) The dynamics of exchange of $\text{N}_\alpha\text{-H}$ with bulk solvent in this and other forms of HRP are under study and will be reported elsewhere.

(26) La Mar, G. N.; de Ropp, J. S.; Budd, D. L.; Kong, S. B.; Smith, K. M.; Langry, K. C., to be published.

(24) La Mar, G. N.; de Ropp, J. S.; Smith, K. M.; Langry, K. C. *J. Biol. Chem.* **1980**, *255*, 1146–1152.

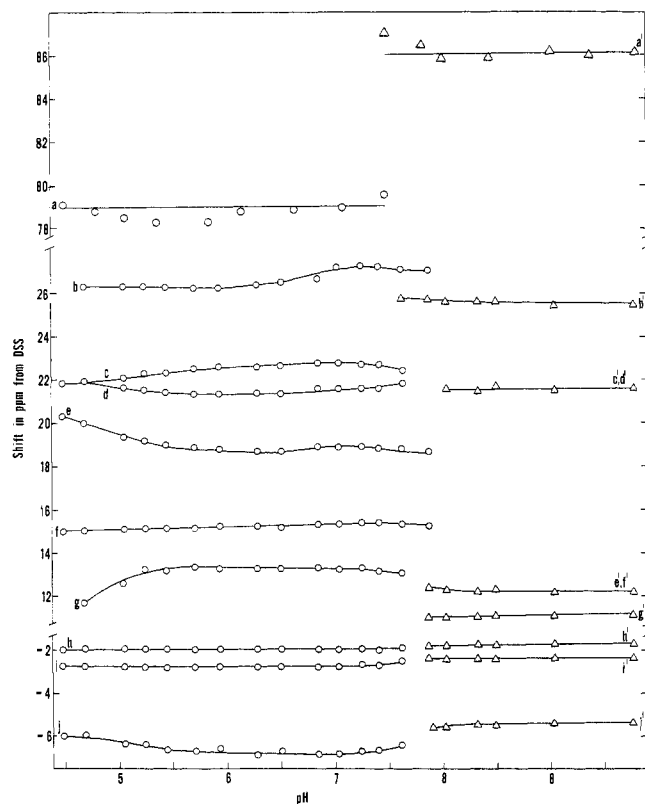


Figure 4. Plot of shifts vs. pH for hyperfine shifted resonances of ferrous HRP at 25 °C, 200 MHz. Peak labeling is the same as in Figure 3.

structure and dictates that the exchangeable peak a, a', as previously found in both models^{15,16} and deoxyhemoproteins,¹⁶⁻¹⁹ arises from the N_{ϵ} -H's of the proximal histidyl imidazole in the two protein conformations. These observations categorically preclude deprotonated proximal histidyl imidazoles in either the neutral or alkaline forms of reduced HRP, in contradiction to indications derived from the interpretation of optical spectra.⁸ The plot of shifts vs. pH for reduced HRP in H₂O at 25 °C is illustrated in Figure 4. There is no evidence for any additional pH dependence for the alkaline form to pH 10. The neutral form displays some curvature for some of the peaks, particularly at very low pH. These effects most likely arise from the titration of the propionic acid side chain.²⁷

The N_{ϵ} H hyperfine shifts, as well as the heme methyl and pyrrole 2,4-H shifts, exhibit magnitudes similar to those found in both models^{15,16} and other deoxyhemoproteins.¹⁶⁻¹⁹ Thus the proximal histidyl imidazole N_{ϵ} H is definitely primarily associated with the imidazole rather than some acceptor residue such as the

(27) The nonexchangeable heme resonances exhibit essentially Curie behavior with apparent intercepts in the diamagnetic region, as also found in deoxy-Mb¹⁹ and monomeric Hb.¹⁸ The exchangeable N_{δ} -H's in both forms also yield apparent intercepts in the diamagnetic region (10 ppm for the acid form and 4 ppm for the alkaline form), though the data for the alkaline form exhibit some curvature at near 0 °C in the direction of larger shifts than expected; we are unable to interpret this small curvature at this time.

glutamate found in the crystal structure of the related cytochrome *c* peroxidase.²⁸ However, the presence of some proton donation by the axial imidazole and hence some partial imidazolate character for the axial ligand are indicated by the changes in the RR $\nu(\text{Fe}-\text{N}_{\delta})$ that has been reported to decrease from 244 to 241 cm^{-1} during the acid \rightarrow alkaline transition.⁹ The larger $\nu(\text{Fe}-\text{N}_{\delta})$ ($\sim 240 \text{ cm}^{-1}$) in reduced HRP relative to that in deoxymyoglobin ($\sim 220 \text{ cm}^{-1}$) already supports a stronger Fe-N₃ bond but does not alone permit differentiation between steric bond compression and H-bonding effects. The N_{ϵ} -H contact shift increases some 7-8 ppm during this same acid-alkaline transition, dictating that the origin of the protein conformational perturbation on the proximal histidine involves electronic changes due to H bonding rather than imposed steric constraints on the iron-imidazole interaction (see Table I). Moreover, we can conclude that the degree of N_{ϵ} -H hydrogen bonding or partial imidazolate character is greater in the acid form than in the alkaline form of the protein. The original⁹ RR data on reduced HRP have also been reinterpreted recently to be consistent with H bonding rather than deprotonation.²⁹

The opposite direction in the changes in $\nu(\text{Fe}-\text{N}_{\delta})$ and N_{ϵ} H contact shift during the structural transition in reduced HRP is contrasted to the behavior found during the T \rightarrow R quaternary transition of tetrameric deoxyhemoglobins. Here the α and β subunits indicate small and moderate increases^{13,14} in $\nu(\text{Fe}-\text{N}_{\delta})$. The N_{ϵ} H contact shifts, however, also decrease during this transition,³⁰ supporting the proposition that the small change in the iron-imidazole bonding characteristic of T \rightarrow R transition is due primarily to steric or strain influences rather than variable H-bonding effects, as suggested recently solely on the basis of RR data.¹⁰

The demonstration that H bonding of the N_{ϵ} H is detectable in HRP but not in myoglobin is consistent with the expectation that more pronounced imidazolate character in the former protein should stabilize the reactive compounds I and II in their proposed iron(IV) states. More quantitative assessment of the degree of H bonding will require the development of a reliable theoretical framework for quantitatively interpreting the hyperfine shifts of coordinated imidazole and imidazolate anions.

Additional support for more extensive imidazolate character for the axial ligand in low-spin ferric HRP relative to metmyoglobins is obtainable from comparing the proximal histidyl imidazole nonexchangeable 2,4-H hyperfine shifts with model compounds containing either an imidazole or imidazolate axial ligand. Details of the methods for locating and assigning these elusive resonances in this protein form will be published elsewhere.³¹

Acknowledgment. This work was supported by grants from the National Institutes of Health, HL-16087 and GM 26226, and the UCD NMR Facility.

Registry No. HRP, 9003-99-0; imidazole, 288-32-4.

(28) Poulos, T. L.; Kraut, J. *J. Biol. Chem.* **1980**, *255*, 8199-8215.

(29) Teroaka, J.; Kitagawa, T. *J. Biol. Chem.* **1981**, *256*, 3969-3977.

(30) Nagai, K.; La Mar, G. N.; Jue, T.; Bunn, H. F. *Biochemistry*, **1982**, *21*, 842-847.

(31) La Mar, G. N.; de Ropp, J. S.; Chacko, V. P., submitted for publication.